

On saturation-strip model of a permeable crack in a piezoelectric ceramic

S. Li, Berkeley, California

Received November 29, 2002; revised June 23, 2003
Published online: October 16, 2003 © Springer-Verlag 2003

Summary. The saturation-strip model for piezoelectric crack is re-examined in a permeable environment to analyze fracture toughness of a piezoelectric ceramic. In this study, a permeable crack is modeled as a vanishing thin but finite rectangular slit with surface charge deposited along crack surfaces. This permeable saturation crack model reveals that there exists a possible leaky mode for electrical field, which allows applied electric field passing through the dielectric medium inside a crack. By taking into account the leaky mode effect, a first-order approximated solution is obtained with respect to slit height, h_0 , in the analysis of electrical and mechanical fields in the vicinity of a permeable crack tip. The permeable saturation crack model presented here also considers the effect of charge distribution on crack surfaces, which may be caused by any possible charge-discharge process in the dielectric medium inside the crack. A closed form solution is obtained for the permeable crack perpendicular to the poling direction under both mechanical as well electrical loads. Both local and global energy release rates are calculated. Remarkably, the global energy release rate for a permeable crack has an expression,

$$J_{cr}^g = \left(\frac{\pi a}{2M} \right) \left(\frac{M\epsilon + \frac{4}{\pi}e^2}{M\epsilon + e^2} \sigma_\infty^2 + \frac{4e}{\pi} \sigma_\infty E_\infty \right),$$

where M is elastic modulus, a is the half crack length, ϵ is permittivity constant, and e is piezoelectric constant. This result is in a broad agreement with some experimental observations and may be served as the fracture criterion for piezoelectric materials. This contribution elucidates how an applied electric field affects crack growth in piezoelectric ceramic through its interaction with permeable environment surrounding a crack.

1 Introduction

Fracture mechanics of piezoelectric solids has been an active research area since early 1990s due to the widespread use of smart materials and smart structures. Many research works have been published in the past decade, e.g., Pak [1, 2], Li et al. [3], Sosa [4], [5], Suo et al. [6, 7], Dunn [8], Dascalu and Maugin [9]–[11], Park and Sun [12], [13], Gao and Barnett [14], and Gao et al. [15], Lynch et al. [16], [17], Zhang and Hack [18], Fulton and Gao [19], Ru [20, 21], Yang and Zhu [22]–[24], Zhang et al. [25], [26], Yang [22], [23] among others. A recent article by Zhang et al. [27] provides a comprehensive review.

A major challenge in fracture mechanics of piezoelectric materials has been how to resolve an outstanding discrepancy between experimental observation and theoretic analysis. In a landmark experimental work done by Park and Sun [12], it was found that the experimental

observation contradicts with some basic aspects of fracture mechanics theory of linear piezoelectric materials. For instance, the experimental results obtained by Park and Sun [12] show that there is a decrease in the critical stress of a cracked piezoelectric body if the electric field is applied along the direction of poling axis, and there is an increase in critical stress if the electric field is applied to the opposite direction, whereas according to linear fracture mechanics theory, the applied electric field does not induce any nonzero stress intensity factor (e.g., Pak [1], [2]; Suo et al. [6]), and it always predicts a negative definite energy release rate regardless the directions of the applied electric fields, which implies that the applied electric field always retards crack growth.

Currently, there are two remedies that have been proposed to explain the discrepancy between linear fracture mechanics theory and experimental observations.

- (i) Yang and Zhu's transformation toughness theory (Yang and Zhu [22]–[24], [28], [29]);
- (ii) Gao et al.'s strip saturation model (Gao et al. [14], [15]) or equivalently, the electric dipole model proposed by Fulton and Gao [19].

From micro-mechanics view point, the so-called *ferroelectric domain switching phenomenon* is the source of nonlinear piezoelectricity (e.g., Yang and Zhu [24], [22], [23], and Sun and Jiang [30]). The explanation is as follows: the concentrated stress field at a crack tip of piezoelectric ceramic will cause depoling, or ferroelectric domain switching, which introduces nonlinear constitutive behaviors, such as a hysteresis loop between the electric displacement and the electric field, and a butterfly loop between the strain and electric field. This will in turn produce toughness variations in ferroelectricity, and alter the constitutive relations at the crack tip region (e.g., Mehta and Vitkar [31]; Sun and Jiang [30]; Zhu and Yang [24]; Yang and Zhu [22], [23]). Thus, the fracture toughness of ferroelectric ceramics may be controlled by domain switching.

Zhu and Yang [24], [23] adopted micromechanics based technique to treat the domain switching induced toughness variation as transformation toughening. At phenomenological level, Gao et al. [15] and Fulton and Gao [19] proposed a strip-saturation model, or the equivalent electric dipole distribution model, to estimate nonlinearity due to the overall effect of domain switching, or polarization. The piezoelectric strip-saturation model is the direct analogous of Dugdale crack in a cohesive elastic medium. Gao and his co-workers [14], [15] showed that a local energy release rate criterion derived from the strip saturation model is in close agreement with the experimental observation, which has become the first theoretical result in this research area that is actually useful.

In this work, a permeable crack model with finite dimension is incorporated with the saturation strip model (Gao et al. [15]) and surface charge distribution to analyze crack growth under possible influences of domain switching effect as well as surface charge-discharge effect. The focuses of this study are:

- (i) Energy release rate of combined saturation strip model and permeable crack model;
- (ii) Crack growth under purely electric loading.

Another outstanding issue in fracture mechanics of piezoelectric materials is crack growth under purely applied electric load. It is the central issue in the theory of ferroelectric fatigue mechanism – a main concern on reliability of many ferroelectric devices, such as non-volatile ferroelectric random access memories (FRAMs). Experimentally, stable crack growths have been observed in both high-cycle fatigue test (Tobin and Park [32]) and low-cycle fatigue test (Cao and Evans [33]; Lynch et al. [16], [17]), under purely electric loading. On the other hand, the linear piezoelectric fracture mechanics predicts a negative definite energy release rate (e.g.,

[1]), which implies that the crack growth should have never occurred under purely electric loading, whereas the nonlinear theory proposed by Gao et al. [15] predicts a positive definite energy release rate regardless whether the direction of applied electric field accords the poling direction or not, which leads to additional paradox: the purely applied electric field that is opposite the poling direction promotes crack growth as well! One of the objectives of this work is to reexamine this important issue. The crack model proposed here takes into account three most important aspects in fracture process in piezoelectric materials: domain switching, permeability, and surface charge distribution. Based on this new crack model, a new solution has been found, which offers a plausible interpretation that is in agreement with experiments.

The presentation is organized in six sections. In Sect. 2, the simplified opening crack model proposed by Gao et al. [15] is briefly outlined within the framework of the permeable crack. The complete solution procedure is provided in Sect. 3, and asymptotic fields of electrical and mechanical variables are documented in Sect. 4. The main results are presented in Sect. 5 focusing on energy release rate of a permeable crack. The crack growth under purely applied electrical load is discussed in Sect. 6. A few remarks are made in the end.

2 Formulation of the problem

2.1 Simplified constitutive model

The notation adopted in this paper follows that of Tiersten [34]. The governing equations for a linear piezoelectric solid are as follows:

Equations of motion

$$\sigma_{ij,i} = 0; \quad (1)$$

Electrostatic charge conservation

$$D_{i,i} = 0; \quad (2)$$

Strain-displacement relations

$$\varepsilon_{ij} = \frac{1}{2}(u_{i,j} + u_{j,i}); \quad (3)$$

Electric field-electric potential relations

$$E_k = -\phi_{,k}; \quad (4)$$

Linear, piezoelectric constitutive relations

$$\sigma_{ij} = c_{ijkl}^E \varepsilon_{kl} - e_{kij} E_k, \quad (5)$$

$$D_i = e_{ikl} \varepsilon_{kl} + \epsilon_{ik}^S E_k, \quad (6)$$

where c_{ijkl}^E are the elastic moduli, e_{kij} are the piezoelectricity coefficients, and ϵ_{ij}^S are the dielectric permittivities (with the superscript E or S indicating material constants measured under conditions of constant electric field or constant strain, respectively).

Using Voigt notation to translate the constitutive relations (5) and (6) into matrix forms, the type of piezoelectric materials that we are interested in can be put into the following form:

$$\begin{bmatrix} \sigma_{11} \\ \sigma_{22} \\ \sigma_{33} \\ \sigma_{23} \\ \sigma_{13} \\ \sigma_{12} \end{bmatrix} = \begin{bmatrix} c_{11}^E & c_{12}^E & c_{13}^E & 0 & 0 & 0 \\ c_{12}^E & c_{11}^E & c_{13}^E & 0 & 0 & 0 \\ c_{13}^E & c_{13}^E & c_{33}^E & 0 & 0 & 0 \\ 0 & 0 & 0 & c_{44}^E & 0 & 0 \\ 0 & 0 & 0 & 0 & c_{44}^E & 0 \\ 0 & 0 & 0 & 0 & 0 & (c_{11}^E - c_{12}^E)/2 \end{bmatrix} \begin{bmatrix} \epsilon_{11} \\ \epsilon_{22} \\ \epsilon_{33} \\ 2\epsilon_{23} \\ 2\epsilon_{13} \\ 2\epsilon_{12} \end{bmatrix} - \begin{bmatrix} 0 & 0 & e_{31} \\ 0 & 0 & e_{31} \\ 0 & 0 & e_{33} \\ 0 & e_{15} & 0 \\ e_{15} & 0 & 0 \\ 0 & 0 & 0 \end{bmatrix} \begin{bmatrix} E_1 \\ E_2 \\ E_3 \end{bmatrix} \quad (7)$$

and

$$\begin{bmatrix} D_1 \\ D_2 \\ D_3 \end{bmatrix} = \begin{bmatrix} 0 & 0 & 0 & 0 & e_{15} & 0 \\ 0 & 0 & 0 & e_{15} & 0 & 0 \\ e_{31} & e_{31} & e_{31} & 0 & 0 & 0 \end{bmatrix} \begin{bmatrix} \epsilon_{11} \\ \epsilon_{22} \\ \epsilon_{33} \\ 2\epsilon_{23} \\ 2\epsilon_{13} \\ 2\epsilon_{12} \end{bmatrix} + \begin{bmatrix} \epsilon_{11}^S & 0 & 0 \\ 0 & \epsilon_{11}^S & 0 \\ 0 & 0 & \epsilon_{33}^S \end{bmatrix} \begin{bmatrix} E_1 \\ E_2 \\ E_3 \end{bmatrix}. \quad (8)$$

Using the precise anisotropic constitutive relation in an analysis often increase the difficulty in finding the closed form solution, or has the danger to obscure the essential physical element of problem. This is true when study a crack with finite height.

Considering the material constants of PZT-4 piezoelectric ceramics used by Park and Sun [12] in their experiment, one may gain a sense of the magnitude of primary material constants.

Elastic constants (N/m^2)

$$\begin{aligned} c_{11}^E &= 13.9 \times 10^{10}, & c_{12}^E &= -7.78 \times 10^{10}, & c_{13}^E &= -7.43 \times 10^{10} \\ c_{33}^E &= 11.3 \times 10^{10}, & c_{44}^E &= 2.56 \times 10^{10} \end{aligned}$$

Piezoelectric constants (C/m^2)

$$e_{31} = -6.98, \quad e_{33} = 13.84, \quad e_{15} = 13.44$$

Dielectric constants (C/Vm)

$$\epsilon_{11}^S = 6.0 \times 10^{-9}, \quad \epsilon_{33}^S = 5.47 \times 10^{-9}$$

In order to simplify analysis, we neglect anisotropic effect and adopt the mode-I GZT (Gao, Zhang, and Tong [15]) crack model, which has the following simplified constitutive relations:

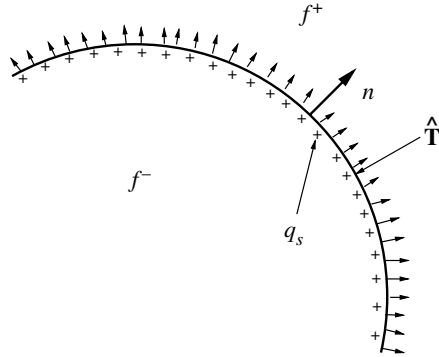


Fig. 1. Convention for boundary conditions

$$\begin{bmatrix} \sigma_{11} \\ \sigma_{22} \\ \sigma_{33} \\ \sigma_{23} \\ \sigma_{13} \\ \sigma_{12} \end{bmatrix} = M \begin{bmatrix} 1 & -1 & -1 & 0 & 0 & 0 \\ -1 & 1 & -1 & 0 & 0 & 0 \\ -1 & -1 & 1 & 0 & 0 & 0 \\ 0 & 0 & 0 & 1 & 0 & 0 \\ 0 & 0 & 0 & 0 & 1 & 0 \\ 0 & 0 & 0 & 0 & 0 & 0 \end{bmatrix} \begin{bmatrix} \epsilon_{11} \\ \epsilon_{22} \\ \epsilon_{33} \\ 2\epsilon_{23} \\ 2\epsilon_{13} \\ 2\epsilon_{12} \end{bmatrix} - e \begin{bmatrix} 0 & 0 & -1 \\ 0 & 0 & -1 \\ 0 & 0 & 1 \\ 0 & 1 & 0 \\ 1 & 0 & 0 \\ 0 & 0 & 0 \end{bmatrix} \begin{bmatrix} E_1 \\ E_2 \\ E_3 \end{bmatrix} \quad (9)$$

and

$$\begin{bmatrix} D_1 \\ D_2 \\ D_3 \end{bmatrix} = e \begin{bmatrix} 0 & 0 & 0 & 0 & 1 & 0 \\ 0 & 0 & 0 & 1 & 0 & 0 \\ -1 & -1 & 1 & 0 & 0 & 0 \end{bmatrix} \begin{bmatrix} \epsilon_{11} \\ \epsilon_{22} \\ \epsilon_{33} \\ 2\epsilon_{23} \\ 2\epsilon_{13} \\ 2\epsilon_{12} \end{bmatrix} + \epsilon \begin{bmatrix} 1 & 0 & 0 \\ 0 & 1 & 0 \\ 0 & 0 & 1 \end{bmatrix} \begin{bmatrix} E_1 \\ E_2 \\ E_3 \end{bmatrix}, \quad (10)$$

where three independent constants, M , e and ϵ are approximation of material constants c_{11}^E, e_{15} and ϵ_{11}^S .

It is believed that the simplified equations, (9) and (10), may capture the essential feature of electrical-mechanical behaviors. In the rest of the paper, we refer this simplified model as the GZT model.

2.2 Boundary conditions

The boundary conditions or interface conditions for two different dielectric media are:

(a) mechanical boundary conditions

$$\mathbf{n} \cdot [[\boldsymbol{\sigma}]] = -\hat{\mathbf{T}} \quad \text{on } S_\sigma; \quad \mathbf{u} = \hat{\mathbf{u}} \quad \text{on } S_u; \quad (11)$$

(b) electrical boundary conditions

$$\mathbf{n} \cdot [[\mathbf{D}]] = q_s \quad \text{and} \quad \mathbf{n} \times [[\mathbf{E}]] = 0 \quad \text{on } S, \quad (12)$$

where S_σ, S_u identify appropriate subsets of the domain boundary and $S = S_\sigma \cup S_u$. Note that the notation $[[f]] := f^+ - f^-$, and the normal vector \mathbf{n} is pointing from medium $-$ to medium $+$.

2.3 Saturation strip model

In this paper, a planar crack is modeled as a vanishing thin, finite dimension, rectangular-shaped slit with height $2h_0$ and width $2a$ as shown in Fig. 2

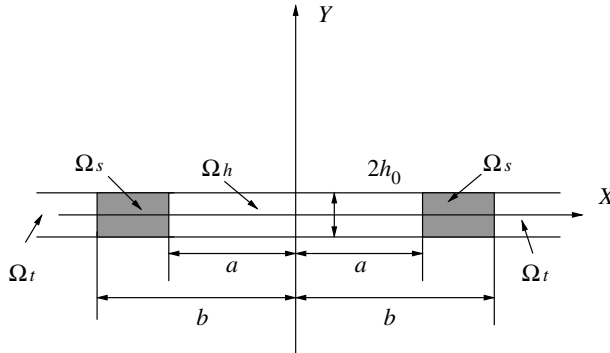


Fig. 2. Geometric configuration of the saturation-strip model

The length of the saturation strip in one side is $b - a$. As $h_0 \rightarrow 0$, the permeable crack becomes a conventional ‘‘Dugdale crack’’ for electrical potential, whereas the length of mechanical crack is always $2a$. One may write crack height as the function of X ,

$$h(X) = \begin{cases} h_0, & |X| < a \\ 0, & |X| > a \end{cases}. \quad (13)$$

The interior region of the crack is denoted as Ω_h ,

$$\Omega_h := \{(X, Y) \mid -a < X < a, \text{ and } -h_0 < Y < h_0\}. \quad (14)$$

The saturation zone is denoted as Ω_s ,

$$\Omega_s := \{(X, Y) \mid a < |X| < b, \text{ and } -h_0 < Y < h_0\}. \quad (15)$$

The adjacent two semi-infinite strip regions to the slit and saturation zone are denoted as Ω_ℓ ,

$$\Omega_\ell := \{(X, Y) \mid b < |X| < \infty, \text{ and } -h_0 < Y < h_0\}. \quad (16)$$

Inside saturation zone, the electric displacement is prescribed

$$D_Y(X, Y) = q_s = \text{const.}, \quad \forall (X, Y) \in \Omega_s. \quad (17)$$

Let $X = x_1, Y = x_3$, and $Z = x_2$ denote regular Cartesian coordinates, where the Y -axis orients in the poling direction. Gao et al. [15] made the following approximations on displacement and electric fields:

$$u_X := u_1 = 0, \quad u_Z := u_2 = 0, \quad \text{and} \quad u_Y = u_3(X, Y) = u(X, Y); \quad (18)$$

$$E_X = E_1 = -\frac{\partial \phi}{\partial X}, \quad E_Z = E_2 = 0, \quad E_Y = E_3 = -\frac{\partial \phi}{\partial Y}. \quad (19)$$

As pointed out by Gao et al. ([15]), the type of approximation adopted here is not new. For instance, it is similar to a simplification made by Rice et al. ([35]) in a study of three-dimensional dynamic crack propagation with a wavy crack front.

Consequently, the governing equations simplify considerably. Constitutive relations (9) and (10) take the form:

$$\sigma_{XX} = -M \frac{\partial u}{\partial Y} - e \frac{\partial \phi}{\partial Y}, \quad (20)$$

$$\sigma_{XY} = M \frac{\partial u}{\partial X} + e \frac{\partial \phi}{\partial X}, \quad (21)$$

$$\sigma_{YY} = M \frac{\partial u}{\partial Y} + e \frac{\partial \phi}{\partial Y}, \quad (22)$$

$$D_X = e \frac{\partial u}{\partial X} - \epsilon \frac{\partial \phi}{\partial X}, \quad (23)$$

$$D_Y = e \frac{\partial u}{\partial Y} - \epsilon \frac{\partial \phi}{\partial Y}. \quad (24)$$

The nontrivial equilibrium equations are:

$$\frac{\partial \sigma_{XX}}{\partial X} + \frac{\partial \sigma_{XY}}{\partial Y} = 0, \quad (25)$$

$$\frac{\partial \sigma_{XY}}{\partial X} + \frac{\partial \sigma_{YY}}{\partial Y} = 0 \quad (26)$$

and electrostatic charge equation becomes

$$\frac{\partial D_X}{\partial X} + \frac{\partial D_Y}{\partial Y} = 0. \quad (27)$$

Substituting Eqs. (20)–(24) into (25)–(27) yields:

$$\begin{aligned} \frac{\partial \sigma_{XX}}{\partial X} + \frac{\partial \sigma_{XY}}{\partial Y} = 0 &\Rightarrow -M \frac{\partial^2 u}{\partial X \partial Y} - e \frac{\partial^2 \phi}{\partial X \partial Y} + M \frac{\partial^2 u}{\partial X \partial Y} + e \frac{\partial^2 \phi}{\partial X \partial Y} = 0, \\ \frac{\partial \sigma_{XY}}{\partial X} + \frac{\partial \sigma_{YY}}{\partial Y} = 0 &\Rightarrow M \nabla^2 u + e \nabla^2 \phi = 0, \end{aligned} \quad (28)$$

$$\frac{\partial D_X}{\partial X} + \frac{\partial D_Y}{\partial Y} = 0 \Rightarrow e \nabla^2 u - \epsilon \nabla^2 \phi = 0, \quad (29)$$

where ∇^2 is the two-dimensional Laplacian operator

$$\nabla^2 := \frac{\partial^2}{\partial X^2} + \frac{\partial^2}{\partial Y^2}.$$

In traditional approach, both u and ϕ can be treated as harmonic functions since $M\epsilon + e^2 \neq 0$, $\nabla^2 u = 0$, $\nabla^2 \phi = 0$, $\forall (X, Y) \in \mathbb{R}^2 / \Omega_h$. (30)

In the interior of a crack, the electric potential satisfies the electrostatic charge equation,

$$\nabla^2 \phi^a = 0, \quad \forall (X, Y) \in \Omega_h, \quad (31)$$

where ϕ^a is the electric potential in the dielectric medium inside a permeable crack, and the superscript a denotes ‘‘air’’.

A slightly different approach is adopted in this paper. Introduce a new electrical potential

$$\psi := \phi - \frac{e}{\epsilon} u. \quad (32)$$

By choosing ψ and u as primary variables, it may be found that

$$e \nabla^2 u - \epsilon \nabla^2 \phi = 0, \quad \rightarrow \quad \nabla^2 \psi = 0, \quad \forall (X, Y) \in \mathbb{R}^2 / \Omega_h, \quad (33)$$

$$M \nabla^2 u + e \nabla^2 \phi = 0, \quad \rightarrow \quad \nabla^2 u = 0, \quad \forall (X, Y) \in \mathbb{R}^2 / \Omega_h. \quad (34)$$

The constitutive relations (20–23) may be rewritten in terms of u and ψ ,

$$\sigma_{XY} = \bar{M} \frac{\partial u}{\partial X} + e \frac{\partial \psi}{\partial X}, \quad (35)$$

$$\sigma_{YY} = \bar{M} \frac{\partial u}{\partial Y} + e \frac{\partial \psi}{\partial Y}, \quad (36)$$

$$D_X = -\epsilon \frac{\partial \psi}{\partial X}, \quad (37)$$

$$D_Y = -\epsilon \frac{\partial \psi}{\partial Y}, \quad (38)$$

where

$$\bar{M} := M + \frac{e^2}{\epsilon}.$$

3 Crack solution

Consider a permeable crack that is perpendicular to the poling direction, and it is subjected to remote traction and charge distribution at remote boundary (see Fig. 3).

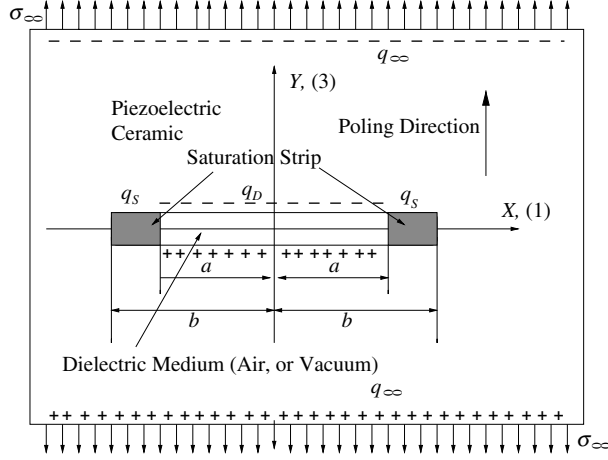


Fig. 3. A permeable crack with saturated tip subjected remote traction and charge loads and charge distribution on the crack surfaces

Let $\hat{\mathbf{T}} = \sigma_\infty \mathbf{e}_Y$ and $q_s = -q_\infty$.

$$\mathbf{n} \cdot [[\boldsymbol{\sigma}]] = -\hat{\mathbf{T}} \rightarrow \sigma_{YY} = \sigma_\infty, \quad \forall Y \rightarrow \infty; \quad (39)$$

$$\mathbf{n} \cdot [[\mathbf{D}]] = q_s \rightarrow D_Y = q_\infty, \quad \forall Y \rightarrow \infty. \quad (40)$$

Assume that due to either discharge of dielectric medium inside a crack, or charge separation due to the newly formed crack surfaces, there is a charge distribution on the entire crack surfaces (see Fig. 3).

The boundary conditions on the crack surfaces,

$$\mathbf{n} \cdot [[\boldsymbol{\sigma}]] = 0, \quad \forall Y = \pm h_0 \quad \text{and} \quad |X| \leq a \quad (41)$$

$$\mathbf{n} \cdot [[\mathbf{D}]] = \mp q_D, \quad \forall Y = \pm h_0 \quad \text{and} \quad |X| \leq a \quad (42)$$

$$\mathbf{n} \times [[\mathbf{E}]] = 0, \quad \forall Y = \pm h_0 \quad \text{and} \quad |X| \leq a \quad (43)$$

which take the form:

$$\sigma_{YY}(X, \pm h_0) = 0, \quad \forall |X| \leq a \quad (44)$$

$$D_Y(X, \pm h_0) - D_Y^a(X, \pm h_0) = \mp q_D, \quad \forall |X| \leq a \quad (45)$$

$$E_X(X, \pm h_0) - E_X^a(X, \pm h_0) = 0, \quad \forall |X| \leq a. \quad (46)$$

In the saturation strip zone,

$$D_Y(X, Y) = q_s, \quad \forall (X, Y) \in \Omega_s, \quad (47)$$

$$u(X, \pm h_0) \approx u(X, 0) = 0, \quad a < |X| < b. \quad (48)$$

And symmetry conditions

$$u(X, 0) = 0, \quad \forall |X| > b \quad (49)$$

$$\phi(X, 0) = 0, \quad \forall |X| > b \quad (50)$$

$$\psi(X, 0) = 0, \quad \forall |X| > b \quad (51)$$

$$\phi^a(X, 0) = 0, \quad \forall 0 < |X| < a \quad (52)$$

or

$$E_X(X, 0) = 0, \quad \forall |X| > a \quad (53)$$

$$E_X^a(X, 0) = 0, \quad \forall 0 < |X| < a. \quad (54)$$

In the dielectric medium inside a permeable crack, $D_i^a = \epsilon_0 E_i^a$ and $E_i^a = -\phi_{,i}^a, i = X, Y$.

Separate displacement and electrical potential fields into two parts: a uniform part due to remote boundary conditions and a disturbance part due to the presence of a crack.

$$u = u_0 + \tilde{u}, \quad (55)$$

$$\phi = \phi_0 + \tilde{\phi}, \quad (56)$$

$$\psi = \psi_0 + \tilde{\psi} \quad (57)$$

and choose

$$u_0 = \mathcal{E}_\infty Y, \quad \phi_0 = -E_\infty Y, \quad \text{and } \psi_0 = -\frac{q_\infty}{\epsilon} Y, \quad (58)$$

where the remote loading parameters are related through

$$\sigma_\infty = M\mathcal{E}_\infty - eE_\infty, \quad q_\infty = e\mathcal{E}_\infty + \epsilon E_\infty, \quad (59)$$

$$\mathcal{E}_\infty = \frac{1}{\Delta_\infty} (\epsilon\sigma_\infty + eq_\infty), \quad E_\infty = \frac{1}{\Delta_\infty} (-e\sigma_\infty + Mq_\infty), \quad (60)$$

where $\Delta_\infty := M\epsilon + e^2$. The above arrangement ensure the conditions that $\tilde{u}, \tilde{\phi}, \tilde{\psi} \rightarrow 0$ as $Y \rightarrow \infty$.

Extend the definition domain of ϕ^a into $\Omega_h \cup \Omega_s \cup \Omega_\ell$ and let

$$\phi^a = \phi_0^a + \tilde{\phi}^a, \quad (61)$$

where the uniform part of the electrical potential is the leaky mode, which is chosen as

$$\phi_0^a = \begin{cases} -\frac{q_\infty}{\epsilon_0} Y, & \forall (X, Y) \in \Omega_h \\ 0, & \forall (X, Y) \in \Omega_s \cup \Omega_\ell \end{cases} \quad (62)$$

and the perturbed part due to the presence of the crack is

$$\tilde{\phi}^a = \begin{cases} \phi^a - \phi_0^a, & \forall (X, Y) \in \Omega_h \\ 0, & \forall (X, Y) \in \Omega_s \cup \Omega_\ell \end{cases}. \quad (63)$$

Introduce Fourier cosine transform

$$\begin{cases} F^*(\zeta, Y) = \sqrt{\frac{2}{\pi}} \int_0^\infty F(X, Y) \cos(\zeta X) dX \\ F(X, Y) = \sqrt{\frac{2}{\pi}} \int_0^\infty F^*(\zeta, Y) \cos(\zeta X) d\zeta \end{cases}, \quad (64)$$

where $F(X, Y) = \tilde{u}(X, Y)$, $\tilde{\phi}(X, Y)$, $\tilde{\psi}(X, Y)$, and $\tilde{\phi}^a(X, Y)$; whereas $F^*(\zeta, Y) = \tilde{u}^*(\zeta, Y)$, $\tilde{\phi}^*(\zeta, Y)$, and $\tilde{\phi}^{a*}(\zeta, Y)$. The transformed governing equations become

$$\frac{d^2}{dY^2} F^* + \zeta^2 F^* = 0. \quad (65)$$

Within the piezoelectric ceramic,

$$\tilde{u}^*(\zeta, Y) = A(\zeta) \exp(-\zeta Y), \quad \forall Y > 0 \quad (66)$$

$$\tilde{\phi}^*(\zeta, Y) = B(\zeta) \exp(-\zeta Y), \quad \forall Y > 0 \quad (67)$$

$$\tilde{\psi}^*(\zeta, Y) = G(\zeta) \exp(-\zeta Y), \quad \forall Y > 0. \quad (68)$$

Inside the permeable crack,

$$\tilde{\phi}^{a*}(\zeta, Y) = C(\zeta) \sinh(\zeta Y), \quad \forall Y > 0 \quad (69)$$

which satisfies the symmetry condition $\tilde{\phi}^a(X, 0) = 0$.

Consider the boundary condition (46),

$$E_X(X, \pm h_0) - E_X^a(X, \pm h_0) = 0, \quad |X| < a \quad (70)$$

and the symmetry condition

$$E_X(X, 0) = 0, \quad |X| > a. \quad (71)$$

On the other hand, in the extended domain

$$E_X^a(X, 0) = 0, \quad |X| > a. \quad (72)$$

Combining Eqs. (70)–(72), one may find

$$\tilde{E}_X(X, \pm h(X)) - \tilde{E}_X^a(X, \pm h(X)) = 0, \quad \forall -\infty < X < +\infty, \quad (73)$$

where function $h(X)$ is defined in Eq. (13).

In transformed space (ζ, Y) , the condition (73) may be approximated as

$$\tilde{E}_X^*(\zeta, \pm h^*(\zeta)) - \tilde{E}_X^{a*}(\zeta, \pm h^*(\zeta)) = 0, \quad \forall 0 < \zeta < +\infty, \quad (74)$$

where

$$h^*(\zeta) = h_0 \frac{\sin(a\zeta)}{\zeta}. \quad (75)$$

Considering Eqs. (67) and (69), one has

$$\begin{aligned} B(\zeta) &= C(\zeta) \frac{1}{2} \left(\exp(2\zeta h^*(\zeta)) - 1 \right) \\ &= C(\zeta) \left(h_0 \sin(a\zeta) + h_0^2 \sin^2(a\zeta) + \frac{2}{3} h_0^3 \sin^3(a\zeta) + \dots \right). \end{aligned} \quad (76)$$

Let

$$B(\zeta) = B_1(\zeta) + h_0 B_2(\zeta) + h_0^2 B_3(\zeta) + \dots \quad (77)$$

By virtue of Eq. (76),

$$B_1(\zeta) = C(\zeta) h_0 \sin(a\zeta), \quad (78)$$

$$B_2(\zeta) = C(\zeta) h_0 \sin^2(a\zeta), \quad (79)$$

$$B_3(\zeta) = C(\zeta) \frac{2h_0}{3} \sin^3(a\zeta), \quad (80)$$

$$\dots \quad (81)$$

Since $h_0 \rightarrow 0$, $\sin(a\zeta)$ is always bounded, the following average approximation is adopted

$$h_0 \sin(a\zeta) \approx h_0 \overline{\sin(a\zeta)} = \sqrt{\frac{\pi}{2}} \frac{h_0}{a}, \quad (82)$$

where

$$\overline{\sin(a\zeta)} := \sqrt{\frac{\pi}{2}} \int_0^\infty \sin(a\zeta) d\zeta = \sqrt{\frac{\pi}{2}} \frac{1}{a}. \quad (83)$$

The equality (83) holds in the sense of generalized function (see, Erdélyi et al. [36] or Lighthill [37], p. 33).

Let

$$r := \sqrt{\frac{2}{\pi}} \frac{a}{h_0}. \quad (84)$$

Equations (81) can then be translated into

$$C(\zeta) = rB_1(\zeta), \quad (85)$$

$$C(\zeta) = r^2 h_0 B_2(\zeta), \quad (86)$$

$$C(\zeta) = \frac{3r^3}{2} h_0^2 B_3(\zeta), \quad (87)$$

$$\dots \quad (88)$$

After Fourier transform, the boundary condition (45) becomes

$$\sqrt{\frac{2}{\pi}} \int_0^\infty \zeta [\epsilon G(\zeta) \exp(-h_0 \zeta) + \epsilon_0 C(\zeta) \cosh(\zeta h_0)] \cos(\zeta X) d\zeta = q_D, \quad \forall 0 < |X| < a. \quad (89)$$

Consider series expansions

$$G(\zeta) = G_1(\zeta) + h_0 G_2(\zeta) + h_0^2 G_3(\zeta) + \dots$$

$$\exp(-h_0 \zeta) = 1 - h_0 \zeta + \frac{(h_0 \zeta)^2}{2!} - \frac{(h_0 \zeta)^3}{3!} + \dots \quad (90)$$

$$\cosh(h_0 \zeta) = 1 + \frac{(h_0 \zeta)^2}{2!} + \frac{(h_0 \zeta)^4}{4!} + \dots \quad (91)$$

Therefore,

$$\begin{aligned} G(\zeta) \exp(-h_0 \zeta) &= G_1(\zeta) + h_0 [-\zeta G_1(\zeta) + G_2(\zeta)] + h_0^2 \left[\frac{\zeta^2}{2!} G_1(\zeta) - \zeta G_2(\zeta) + G_3(\zeta) \right] \\ &\quad + h_0^3 \left[-\frac{\zeta^3}{3!} G_1(\zeta) + \frac{\zeta^2}{2!} G_2(\zeta) - \zeta G_3(\zeta) + G_4(\zeta) \right] + \dots \end{aligned} \quad (92)$$

and

$$C(\zeta) \cosh(\zeta h_0) = rB_1(\zeta) + h_0^2 r \left(\frac{\zeta^2}{2!} B_1(\zeta) \right) + h_0^4 r \left(\frac{\zeta^4}{4!} B_1(\zeta) \right) + \dots \quad (93)$$

Throughout this paper, it is assumed that the product $\epsilon_0 r$ is bounded, i.e. $\epsilon_0 r < C$, $C > 0$, and C is independent with r or ϵ_0 . When approaching to the impermeable limit, $\epsilon_0 r \rightarrow 0$.

The following asymptotic integral equation series may then be derived, $\forall 0 < X < a$:

$$h_0^0 : \sqrt{\frac{2}{\pi}} \int_0^\infty \zeta [\epsilon G_1(\zeta) + \epsilon_0 r B_1(\zeta)] \cos(\zeta X) d\zeta = -q_D, \quad (94)$$

$$h_0^1 : \sqrt{\frac{2}{\pi}} \int_0^\infty \zeta [-\zeta G_1(\zeta) + G_2(\zeta)] \cos(\zeta X) d\zeta = 0, \quad (95)$$

$$h_0^2 : \sqrt{\frac{2}{\pi}} \int_0^\infty \zeta \left\{ \epsilon \left(\frac{\zeta^2}{2} G_1(\zeta) - \zeta G_2(\zeta) + G_3(\zeta) \right) + \epsilon_0 r \zeta^2 B_1(\zeta) \right\} \cos(\zeta X) d\zeta = 0, \dots \quad (96)$$

The saturation condition, $D_Y(X, h_0) = q_S$, provides additional boundary condition in $a < |X| < b$. That is

$$\sqrt{\frac{2}{\pi}} \int_0^{\infty} \epsilon \zeta G(\zeta) \exp(-h_0 \zeta) \cos(\zeta X) d\zeta = q_S - q_{\infty}. \quad (97)$$

The asymptotic expansion gives

$$\begin{aligned} h_0^0 &: \sqrt{\frac{2}{\pi}} \int_0^{\infty} \zeta G_1(\zeta) \cos(\zeta X) d\zeta = \frac{q_S - q_{\infty}}{\epsilon}, \\ h_0^1 &: \sqrt{\frac{2}{\pi}} \int_0^{\infty} \zeta [-\zeta G_1(\zeta) + G_2(\zeta)] \cos(\zeta X) d\zeta = 0, \\ h_0^2 &: \sqrt{\frac{2}{\pi}} \int_0^{\infty} \zeta \left[\frac{\zeta^2}{2} G_1(\zeta) - \zeta G_2(\zeta) + G_3(\zeta) \right] \cos(\zeta X) d\zeta = 0 \dots \end{aligned} \quad (98)$$

Consider that $\phi^*(\zeta, Y) = \psi^*(\zeta, Y) + \frac{e}{\epsilon} u^*(\zeta, Y)$, which leads to

$$B(\zeta) = G(\zeta) + \frac{e}{\epsilon} A(\zeta). \quad (99)$$

Let

$$A(\zeta) = A_1(\zeta) + h_0 A_2(\zeta) + h_0^2 A_3(\zeta) + \dots \quad (100)$$

The first-order approximation of electric displacement boundary condition can be expressed in the following integral form:

$$\begin{aligned} \sqrt{\frac{2}{\pi}} \int_0^{\infty} \zeta \left[(\epsilon + \epsilon_0 r) G_1(\zeta) + \frac{\epsilon_0 r e}{\epsilon} A_1(\zeta) \right] \cos(\zeta X) d\zeta &= q_D, \quad |X| < a, \\ \sqrt{\frac{2}{\pi}} \int_0^{\infty} \zeta G_1(\zeta) \cos(\zeta X) d\zeta &= \frac{q_S - q_{\infty}}{\epsilon}, \quad a < |X| < b. \end{aligned} \quad (101)$$

The integral form of the stress-free boundary condition on crack surfaces is

$$\begin{aligned} \sigma_Y(X, h_0) &= \sigma_{\infty} - \bar{M} \sqrt{\frac{2}{\pi}} \int_0^{\infty} \zeta A(\zeta) \cos(\zeta X) \exp(-h_0 \zeta) d\zeta \\ &\quad + e \sqrt{\frac{2}{\pi}} \int_0^{\infty} \zeta G(\zeta) \cos(\zeta X) \exp(-h_0 \zeta) d\zeta = 0, \quad |X| < a. \end{aligned} \quad (102)$$

For $|X| < a$, asymptotic expansion gives

$$\begin{aligned} h_0^0 &: \sqrt{\frac{2}{\pi}} \int_0^{\infty} \zeta \left[\bar{M} A_1(\zeta) - e G_1(\zeta) \right] \cos(\zeta X) d\zeta = \sigma_{\infty}, \\ h_0^1 &: \sqrt{\frac{2}{\pi}} \int_0^{\infty} \zeta \left\{ \bar{M} \left[-\zeta A_1(\zeta) + A_2(\zeta) \right] - e \left[-\zeta G_1(\zeta) + G_2(\zeta) \right] \right\} \cos(\zeta X) d\zeta = 0, \\ h_0^2 &: \sqrt{\frac{2}{\pi}} \int_0^{\infty} \zeta \left\{ \bar{M} \left[\frac{\zeta^2}{2!} A_1(\zeta) - \zeta A_2(\zeta) + A_3(\zeta) \right] - e \left[\frac{\zeta^2}{2!} G_1(\zeta) - \zeta G_2(\zeta) + G_3(\zeta) \right] \right\} \cos(\zeta X) d\zeta = 0, \\ &\dots \end{aligned} \quad (103)$$

Consider symmetry condition

$$u(X, 0) = 0, \quad |X| > a \quad (104)$$

and note that inside the saturation zone,

$$u(X, 0) = 0, \quad \forall a < |X| < b \quad (105)$$

is assumed.

For electrical potentials, symmetry condition gives

$$\phi(X, 0) = 0, \quad \text{and} \quad \psi(X, 0) = 0, \quad \forall |X| > b. \quad (106)$$

They lead to

$$\sqrt{\frac{2}{\pi}} \int_0^{\infty} A_i(\zeta) \cos(\zeta X) d\zeta = 0, \quad \forall |X| > a, \quad (107)$$

$$\sqrt{\frac{2}{\pi}} \int_0^{\infty} G_i(\zeta) \cos(\zeta X) d\zeta = 0, \quad \forall |X| > b, \quad (108)$$

for $i = 1, 2, \dots$

By combining Eqs. (94)–(96) and Eqs. (107)–(108), the complete first-order integral equations for the mixed boundary value problem are found as

$$\begin{aligned} \sqrt{\frac{2}{\pi}} \int_0^{\infty} \zeta \left[\bar{M}A_1(\zeta) - eG_1(\zeta) \right] \cos(\zeta X) d\zeta &= \sigma_{\infty}, \quad |X| < a \\ \sqrt{\frac{2}{\pi}} \int_0^{\infty} \zeta \left[\frac{\epsilon_0 r e}{\epsilon} A_1(\zeta) + (\epsilon + \epsilon_0 r) G_1(\zeta) \right] \cos(\zeta X) d\zeta &= -q_D, \quad |X| < a \\ \sqrt{\frac{2}{\pi}} \int_0^{\infty} \zeta G_1(\zeta) \cos(\zeta X) d\zeta &= \frac{q_S - q_{\infty}}{\epsilon}, \quad a < |X| < b \\ \sqrt{\frac{2}{\pi}} \int_0^{\infty} A_1(\zeta) \cos(\zeta X) d\zeta &= 0, \quad \forall |X| > a \\ \sqrt{\frac{2}{\pi}} \int_0^{\infty} G_1(\zeta) \cos(\zeta X) d\zeta &= 0, \quad \forall |X| > b \end{aligned} \quad (109)$$

which may be reduced to two sets of dual integral equations

$$\left\{ \begin{aligned} \sqrt{\frac{2}{\pi}} \int_0^{\infty} \zeta A_1(\zeta) \cos(\zeta X) d\zeta &= \sigma(X), \quad |X| < a \\ \sqrt{\frac{2}{\pi}} \int_0^{\infty} A_1(\zeta) \cos(\zeta X) d\zeta &= 0, \quad |X| > a \end{aligned} \right. , \quad (110)$$

$$\begin{cases} \sqrt{\frac{2}{\pi}} \int_0^\infty \zeta G_1(\zeta) \cos(\zeta X) d\zeta = q(X), & |X| < b \\ \sqrt{\frac{2}{\pi}} \int_0^\infty G_1(\zeta) \cos(\zeta X) d\zeta = 0, & |X| > b \end{cases}, \quad (111)$$

where

$$\sigma(X) = \frac{1}{\Delta_c} [(\epsilon + \epsilon_0 r) \sigma_\infty + e q_D], \quad |X| < a, \quad (112)$$

$$q(X) = -\frac{1}{\Delta_c} \left[\bar{M} q_D + \left(\frac{\epsilon_0 r e}{\epsilon} \right) \sigma_\infty \right] (H(X) - H(X - a)) + \frac{(q_s - q_\infty)}{\epsilon} H(X - a), \quad 0 < |X| < b, \quad (113)$$

where $\Delta_c := M(\epsilon + \epsilon_0 r) + e^2$ and $H(X)$ is standard Heaviside function.

Let

$$A_1(\zeta) = \sqrt{\frac{\pi}{2}} \int_0^b f(t) t J_0(\zeta t) dt, \quad (114)$$

$$G_1(\zeta) = \sqrt{\frac{\pi}{2}} \int_0^b g(t) t J_0(\zeta t) dt, \quad (115)$$

where $f(t)$ and $g(t)$ are unknown functions, and

$$\sqrt{\frac{2}{\pi}} \int_0^\infty A_1(\zeta) \cos(\zeta X) d\zeta = \begin{cases} \int_X^b \frac{f(t)t}{\sqrt{t^2 - X^2}} dt, & |X| < a \\ 0, & |X| > a \end{cases}, \quad (116)$$

$$\sqrt{\frac{2}{\pi}} \int_0^\infty G_1(\zeta) \cos(\zeta X) d\zeta = \begin{cases} \int_X^b \frac{g(t)t}{\sqrt{t^2 - X^2}} dt, & |X| < b \\ 0, & |X| > b \end{cases}. \quad (117)$$

The dual integral equations (110)–(111) are then reduced to a set of Abel integral equations

$$\frac{d}{dX} \int_0^X \begin{pmatrix} f(t) \\ g(t) \end{pmatrix} \frac{tdt}{\sqrt{X^2 - t^2}} = \begin{pmatrix} \sigma(X) \\ q(X) \end{pmatrix}. \quad (118)$$

Following the standard procedure (e.g., Sneddon and Lowengrub [38]), one may find that

$$f(t) = \frac{2}{\pi} \int_0^t \frac{\sigma(X)}{\sqrt{t^2 - X^2}} dX = \frac{1}{\Delta_c} [(\epsilon + \epsilon_0 r) + e q_D] \sigma_\infty, \quad 0 < t < a, \quad (119)$$

$$\begin{aligned} g(t) &= \frac{2}{\pi} \int_0^t \frac{q(X)}{\sqrt{t^2 - X^2}} dX = -\frac{1}{\Delta_c} \left[\bar{M} q_D + \left(\frac{\epsilon_0 r e}{\epsilon} \right) \sigma_\infty \right] \\ &\quad + \left\{ \frac{1}{\epsilon} (q_s - q_\infty) + \frac{1}{\Delta_c} \left[\bar{M} q_D + \left(\frac{\epsilon_0 r e}{\epsilon} \right) \sigma_\infty \right] \right\} \cdot \left(\frac{2}{\pi} \right) \cos^{-1} \left(\frac{a}{t} \right) H(t - a), \quad 0 < t < b. \end{aligned} \quad (120)$$

Subsequently, the displacement and electric potential along crack surfaces can be found as well,

$$u(X, h_0) \approx \int_X^a \frac{f(t)t}{\sqrt{t^2 - X^2}} dt = \frac{1}{\Delta_c} [(\epsilon + \epsilon_0 r) + e q_D] \sigma_\infty \sqrt{a^2 - X^2}, \quad \forall |X| < a, \quad (121)$$

$$\begin{aligned} \psi(X, h_0) \approx \int_X^b \frac{g(t)t}{\sqrt{t^2 - X^2}} dt = & \left\{ -\frac{1}{\Delta_c} [\bar{M} q_D + \left(\frac{\epsilon_0 r e}{\epsilon}\right) \sigma_\infty] + \left(\frac{\theta}{\pi/2}\right) \left[\left(\frac{q_S - q_\infty}{\epsilon}\right) \right. \right. \\ & \left. \left. + \frac{1}{\Delta_c} (\bar{M} q_D + \left(\frac{\epsilon_0 r e}{\epsilon}\right) \sigma_\infty) \right] \right\} \sqrt{b^2 - X^2} - \left(\frac{1}{\pi}\right) \left(\frac{q_S - q_\infty}{\epsilon} + \frac{1}{\Delta_c} [\bar{M} q_D + \left(\frac{\epsilon_0 r e}{\epsilon}\right) \sigma_\infty] \right) \\ & \cdot \left\{ X \ln \left| \frac{a\sqrt{b^2 - X^2} - X\sqrt{b^2 - a^2}}{X\sqrt{b^2 - a^2} + a\sqrt{b^2 - X^2}} \right| + a \ln \left| \frac{\sqrt{b^2 - a^2} - \sqrt{b^2 - X^2}}{\sqrt{b^2 - a^2} + \sqrt{b^2 - X^2}} \right| \right\} \quad \forall |X| < b. \quad (122) \end{aligned}$$

By virtue of the identity

$$\phi = \psi + \frac{e}{\epsilon} u,$$

$$\begin{aligned} \phi(X, h_0) \approx \frac{e}{\epsilon \Delta_c} [(\epsilon + \epsilon_0 r) + e q_D] \sigma_\infty \sqrt{a^2 - X^2} (H(X) - H(X - a)) \\ + \left\{ -\frac{1}{\Delta_c} [\bar{M} q_D + \left(\frac{\epsilon_0 r e}{\epsilon}\right) \sigma_\infty] + \left(\frac{\theta}{\pi/2}\right) \left[\left(\frac{q_S - q_\infty}{\epsilon}\right) \right. \right. \\ \left. \left. + \frac{1}{\Delta_c} (\bar{M} q_D + \left(\frac{\epsilon_0 r e}{\epsilon}\right) \sigma_\infty) \right] \right\} \sqrt{b^2 - X^2} (H(X) - H(X - b)) \\ - \left(\frac{1}{\pi}\right) \left(\frac{q_S - q_\infty}{\epsilon} + \frac{1}{\Delta_c} [\bar{M} q_D + \left(\frac{\epsilon_0 r e}{\epsilon}\right) \sigma_\infty] \right) \cdot \left\{ X \ln \left| \frac{a\sqrt{b^2 - X^2} - X\sqrt{b^2 - a^2}}{X\sqrt{b^2 - a^2} + a\sqrt{b^2 - X^2}} \right| \right. \\ \left. + a \ln \left| \frac{\sqrt{b^2 - a^2} - \sqrt{b^2 - X^2}}{\sqrt{b^2 - a^2} + \sqrt{b^2 - X^2}} \right| \right\} (H(X) - H(X - b)), \quad (123) \end{aligned}$$

where

$$\theta = \cos^{-1} \left(\frac{a}{b} \right).$$

The gradient fields for both vertical displacement and electrical potentials along the upper crack surface line are given as follows:

$$\frac{\partial u}{\partial Y}(X, h_0) \approx \begin{cases} \mathcal{E}_\infty - \frac{1}{\Delta_c} [(\epsilon + \epsilon_0 r) \sigma_\infty + e q_D], & |X| < a \\ \mathcal{E}_\infty - \frac{1}{\Delta_c} [(\epsilon + \epsilon_0 r) \sigma_\infty + e q_D] \left[1 - \frac{X}{\sqrt{X^2 - a^2}} \right], & |X| > a \end{cases}. \quad (124)$$

To eliminate the singularity of electrical displacement field, the following saturation condition has to be satisfied at the tip of the saturation zone,

$$\left\{ -\frac{1}{\Delta_c} [\bar{M} q_D + \left(\frac{\epsilon_0 r e}{\epsilon}\right) \sigma_\infty] + \left(\frac{\theta}{\pi/2}\right) \left[\left(\frac{q_S - q_\infty}{\epsilon}\right) + \frac{1}{\Delta_c} (\bar{M} q_D + \left(\frac{\epsilon_0 r e}{\epsilon}\right) \sigma_\infty) \right] \right\} = 0, \quad (125)$$

where

$$\theta = \cos^{-1}\left(\frac{a}{b}\right).$$

From Eq. (125), one may be able to determine the size of saturation zone,

$$\theta = \cos^{-1}\left(\frac{a}{b}\right) = \left(\frac{\pi}{2}\right) \frac{\frac{1}{\Delta_c} \left[\bar{M}q_D + \left(\frac{\epsilon_0 r e}{\epsilon}\right) \sigma_\infty \right]}{\left(\frac{q_S - q_\infty}{\epsilon}\right) + \frac{1}{\Delta_c} \left[\bar{M}q_D + \left(\frac{\epsilon_0 r e}{\epsilon}\right) \sigma_\infty \right]}. \quad (126)$$

Let $\epsilon_0 = 0$ and $q_D = q_\infty$. We recover the original saturation-strip solution obtained by Gao et al. [15] under the impermeable assumption,

$$\theta = \left(\frac{\pi}{2}\right) \frac{q_\infty}{q_S}. \quad (127)$$

From the above analysis, one may find that simply setting $\epsilon_0 = 0$ is not enough to recover the impermeable solution. Instead, it involves a complete discharge process on crack surfaces, which has to block the passage of applied electrical field completely to suppress the leaky mode. On the other hand, if there is no charge distribution along crack surfaces, $q_D = 0$, and $\epsilon_0 = 0$, the piezoelectric material in front of the crack tip may not be able to be saturated, because $\theta = 0 \rightarrow a = b$.

In reality, any amount the negative charge distribution along the upper half of the crack surface may represent a partial discharge, shielding the dielectric medium inside the crack from the applied electrical field. For the saturation zone with fixed size, the intensity of charge distribution along crack surfaces can be determined by the following expression:

$$q_D = \frac{\Delta_c \bar{\theta}}{\bar{M}(1 - \bar{\theta})} \left(\frac{q_S - q_\infty}{\epsilon}\right) - \left(\frac{\epsilon_0 r e}{\epsilon \bar{M}}\right) \sigma_\infty, \quad (128)$$

where $\bar{\theta} = \theta/(\pi/2)$.

The gradient of electric potentials are

$$\frac{\partial \psi}{\partial Y}(X, h_0) = \begin{cases} -\left(\frac{q_\infty}{\epsilon} - \frac{1}{\Delta_c} \left[\bar{M}q_D + \left(\frac{\epsilon_0 r e}{\epsilon}\right) \sigma_\infty \right]\right), & 0 < |X| < a \\ -\frac{q_S}{\epsilon}, & a < |X| < b \\ -\left(\frac{q_\infty}{\epsilon} - \frac{1}{\Delta_c} \left[\bar{M}q_D + \left(\frac{\epsilon_0 r e}{\epsilon}\right) \sigma_\infty \right]\right) \\ + \text{higher-order terms} & |X| > b \end{cases} \quad (129)$$

and

$$\frac{\partial \phi}{\partial Y} = \begin{cases} -E_\infty + \frac{1}{\Delta_c} \left[Mq_D - e\sigma_\infty \right], & |X| < a \\ -\frac{q_S}{\epsilon} + \frac{e}{\epsilon} \left[\mathcal{E}_\infty - \frac{1}{\Delta_c} (\epsilon + \epsilon_0 r) \sigma_\infty + eq_D \right] \\ + \frac{e}{\epsilon \Delta_c} \left[(\epsilon + \epsilon_0 r) \sigma_\infty + eq_D \right] \frac{X}{\sqrt{X^2 - a^2}}, & a < |X| < b \\ -E_\infty + \frac{1}{\Delta_c} \left[Mq_D - e\sigma_\infty \right] \\ + \frac{e}{\epsilon \Delta_c} \left[(\epsilon + \epsilon_0 r) \sigma_\infty + eq_D \right] \frac{X}{\sqrt{X^2 - a^2}} \\ + \text{higher-order terms}, & |X| > b. \end{cases} \quad (130)$$

4 Asymptotic fields and intensity factors

To measure the local mechanical and electrical fields in front a crack tip, intensity factors are derived for the relevant field variables. At $Y = 0$, the general forms of asymptotic fields of both mechanical and electric variables in front of the crack tip can be found as follows:

$$\epsilon_{YY} = \frac{1}{\Delta_c} \left((\epsilon + \epsilon_0 r) \sigma_\infty + eq_D \right) \frac{X}{\sqrt{X^2 - a^2}} + \left(\mathcal{E}_\infty - \frac{1}{\Delta_c} \left[(\epsilon + \epsilon_0 r) \sigma_\infty + eq_D \right] \right), \quad (131)$$

$$E_Y = - \left(\frac{e}{\epsilon \Delta_c} \right) \left((\epsilon + \epsilon_0 r) \sigma_\infty + eq_D \right) \frac{X}{\sqrt{X^2 - a^2}} + \frac{q_S}{\epsilon} + \frac{e}{\epsilon \Delta_c} \left((\epsilon + \epsilon_0 r) \sigma_\infty + eq_D - \mathcal{E}_\infty \Delta_c \right), \quad (132)$$

$$\sigma_{YY} = \frac{\bar{M}}{\Delta_c} \left((\epsilon + \epsilon_0 r) \sigma_\infty + eq_D \right) \frac{X}{\sqrt{X^2 - a^2}} + \bar{M} \left(\mathcal{E}_\infty - \frac{1}{\Delta_c} \left[(\epsilon + \epsilon_0 r) \sigma_\infty + eq_D \right] \right) - \frac{eq_S}{\epsilon}, \quad (133)$$

$$D_Y = q_S. \quad (134)$$

The relevant field intensity factors can be found as follows:

$$K_I^S = \lim_{X \rightarrow a^+} \sqrt{2\pi(X-a)} \epsilon_{YY}(X, 0) = \left((\epsilon + \epsilon_0 r) \sigma_\infty + eq_D \right) \frac{\sqrt{\pi a}}{\Delta_c}, \quad (135)$$

$$K_I^E = \lim_{X \rightarrow a^+} \sqrt{2\pi(X-a)} E_Y(X, 0) = - \left((\epsilon + \epsilon_0 r) \sigma_\infty + eq_D \right) \frac{e}{\epsilon \Delta_c} \sqrt{\pi a}, \quad (136)$$

$$K_I^T = \lim_{X \rightarrow a^+} \sqrt{2\pi(X-a)} \sigma_{YY}(X, 0) = \bar{M} \left((\epsilon + \epsilon_0 r) \sigma_\infty + eq_D \right) \frac{\sqrt{\pi a}}{\Delta_c}, \quad (137)$$

$$K_I^D = \lim_{X \rightarrow a^+} \sqrt{2\pi(X-a)} D_Y(X, 0) = 0. \quad (138)$$

A few special cases are deserved special attentions.

4.1 Without surface charge

Assume that there is no surface charge on the crack surfaces. Let $q_D = 0$. The asymptotic fields become:

$$\epsilon_{YY} = \frac{1}{\Delta_c} \left(\epsilon + \epsilon_0 r \right) \sigma_\infty \frac{X}{\sqrt{X^2 - a^2}} + \left(\mathcal{E}_\infty - \frac{1}{\Delta_c} \left((\epsilon + \epsilon_0 r) \sigma_\infty \right) \right), \quad (139)$$

$$E_Y = - \left(\frac{e}{\epsilon \Delta_c} \right) \left((\epsilon + \epsilon_0 r) \sigma_\infty \frac{X}{\sqrt{X^2 - a^2}} + \frac{q_S}{\epsilon} + \frac{e}{\epsilon \Delta_c} \left((\epsilon + \epsilon_0 r) \sigma_\infty - \mathcal{E}_\infty \Delta_c \right) \right), \quad (140)$$

$$\sigma_{YY} = \frac{\bar{M}}{\Delta_c} \left(\epsilon + \epsilon_0 r \right) \sigma_\infty \frac{X}{\sqrt{X^2 - a^2}} + \bar{M} \left(\mathcal{E}_\infty - \frac{1}{\Delta_c} \left((\epsilon + \epsilon_0 r) \sigma_\infty \right) \right) - \frac{eq_S}{\epsilon}, \quad (141)$$

$$D_Y = q_S \quad (142)$$

and the related intensity factors are

$$K_I^S = \frac{\sqrt{\pi a}}{\Delta_c} (\epsilon + \epsilon_0 r) \sigma_\infty, \quad (143)$$

$$K_I^E = -\frac{\sqrt{\pi a} e}{\epsilon \Delta_c} (\epsilon + \epsilon_0 r) \sigma_\infty, \quad (144)$$

$$K_I^T = \frac{\sqrt{\pi a} \bar{M}}{\Delta_c} (\epsilon + \epsilon_0 r) \sigma_\infty, \quad (145)$$

$$K_I^D = 0. \quad (146)$$

They are not affected by remote electric loading as well as domain switching induced saturation.

Furthermore, let $\epsilon_0 = 0$, and $\Delta_c = \Delta_\infty$. We recover the results obtained by Zhang and Hack [18] for a mode III crack in linear media,

$$K_I^S = \frac{\epsilon}{\Delta_\infty} \sigma_\infty \sqrt{\pi a}, \quad (147)$$

$$K_I^E = -\frac{e}{\Delta_\infty} \sigma_\infty \sqrt{\pi a}, \quad (148)$$

$$K_I^T = \sigma_\infty \sqrt{\pi a}, \quad (149)$$

$$K_I^D = 0. \quad (150)$$

4.2 Zero crack height solution ($h_0 = 0$)

Let $h_0 = 0$ and consequently $r \rightarrow \infty$. That is: the slit has zero height. The physical interpretation of this limit is that the upper and lower crack surfaces are in close contact during fracture process. Therefore, there is no dielectric medium inside the crack. The asymptotic fields become:

$$\epsilon_{YY} = \frac{\sigma_\infty}{M} \frac{X}{\sqrt{X^2 - a^2}} + \left(\epsilon_\infty - \frac{\sigma_\infty}{M} \right), \quad (151)$$

$$E_Y = -\left(\frac{e \sigma_\infty}{M \epsilon} \right) \frac{X}{\sqrt{X^2 - a^2}} + \left(\frac{q_S}{\epsilon} - \frac{e^2}{\epsilon M} E_\infty \right), \quad (152)$$

$$\sigma_{YY} = \frac{\bar{M}}{M} \sigma_\infty \frac{X}{\sqrt{X^2 - a^2}} + \frac{\bar{M}}{M} e E_\infty - \frac{e}{\epsilon} q_S, \quad (153)$$

$$D_Y = q_S. \quad (154)$$

4.3 Impermeable solution

Since $\epsilon_0 \ll 1$ in reality, we consider the crack solution in the impermeable limit, $\epsilon_0 r \rightarrow 0$. In this case, $\Delta_c \rightarrow \Delta_\infty = M\epsilon + e^2$. The asymptotic solution in a permeable and saturated crack front is

$$\epsilon_{YY} = \frac{(\epsilon \sigma_\infty + e q_D)}{\Delta_\infty} \frac{X}{\sqrt{X^2 - a^2}} + \frac{e}{\Delta_\infty} (q_\infty - q_D), \quad (155)$$

$$E_Y = -\left(\frac{e}{\epsilon} \right) \frac{(\epsilon \sigma_\infty + e q_D)}{\Delta_\infty} \frac{X}{\sqrt{X^2 - a^2}} + \frac{q_S}{\epsilon} + \frac{e^2}{\epsilon} \frac{1}{\Delta_\infty} (q_D - q_\infty), \quad (156)$$

$$\sigma_{YY} = \left(\sigma_\infty + \frac{e}{\epsilon} q_D \right) \frac{X}{\sqrt{X^2 - a^2}} + \frac{e}{\epsilon} (q_\infty - q_S - q_D), \quad (157)$$

$$D_Y = q_S. \quad (158)$$

Consider the complete discharge process, i.e. the charge distribution on crack surfaces is prescribed as $q_D = q_\infty$. The asymptotic fields in front of the crack tip become:

$$\epsilon_{YY} = \mathcal{E}_\infty \frac{X}{\sqrt{X^2 - a^2}}, \quad (159)$$

$$E_Y = -\left(\frac{e}{\epsilon}\right) \mathcal{E}_\infty \frac{X}{\sqrt{X^2 - a^2}} + \frac{q_S}{\epsilon}, \quad (160)$$

$$\sigma_Y = \frac{\mathcal{E}_\infty \Delta_\infty}{\epsilon} \frac{X}{\sqrt{X^2 - a^2}} - \frac{e}{\epsilon} q_S, \quad (161)$$

$$D_Y = q_S. \quad (162)$$

These results recover exactly the GZT crack solution obtained by Gao et al [15] under the impermeable assumption. *This result unveils that the so-called impermeable solution is more than just an approximation by setting $\epsilon_0 = 0$. It is involved a complete dis-charge process on crack surface to shield off the interaction between the dielectric medium inside a crack and the piezo-electric matrix.*

The relevant field intensity factors can be found as follows:

$$K_I^S = \sqrt{\pi a} \mathcal{E}_\infty, \quad (163)$$

$$K_I^E = -\sqrt{\pi a} \left(\frac{e}{\epsilon}\right) \mathcal{E}_\infty, \quad (164)$$

$$K_I^T = \sqrt{\pi a} \frac{\Delta_\infty}{\epsilon} \mathcal{E}_\infty, \quad (165)$$

$$K_I^D = 0, \quad (166)$$

where the remote applied electric field strength may be expressed as

$$\mathcal{E}_\infty = \frac{1}{M} \left(\sigma_\infty + eE_\infty \right). \quad (167)$$

5 Energy release rate

The expression of J -integral in a piezoelectric medium is given by Cherepanov [39],

$$J = \int_{\Gamma} \left(H n_X - \sigma_{ij} n_i u_{j,X} - n_i D_i \phi_{,X} \right) dS, \quad (168)$$

where H is the electric enthalpy density.

For permeable cracks, J -integral has two parts: *Local energy release rate*, and *Global energy release rate*. The so-called local energy release rate is defined as the contour integral, J , along an infinitesimal circle around the crack tip, Γ_ℓ ; *Global energy release rate*, which may be defined as any contour integral, J , starting at the center of the lower part of the crack surface and ending at the center of upper part of the crack surface (see Fig. 4). The total energy release rate, or the so-called global energy release rate, is the sum of the local energy release rate and the contour integral contribution along the crack surfaces, i.e.,

$$J_g = J_\ell + J_{cs}, \quad (169)$$

where J_{cs} denote the energy release rate contribution from crack surfaces.

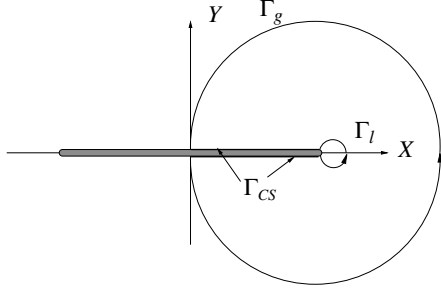


Fig. 4. J -integral contours for evaluating local and global energy release rates

Arguments have been made by Gao and his colleagues [14, 15] about different roles that local and global energy release rates may play in the process of piezoelectric fracture.

The local energy release rate can be calculated by the following expression:

$$J_\ell = \frac{1}{2} \left(K_I^S K_I^T - K_I^E K_I^D \right) = \frac{1}{2} \left\{ \left[(\epsilon + \epsilon_0 r) \sigma_\infty + e q_D \right]^2 \left(\frac{\pi a}{\Delta_c^2} \right) \bar{M} \right\}, \quad (170)$$

when $\epsilon_0 = 0$,

$$J_\ell = \frac{1}{2} \frac{\pi a}{\epsilon \Delta_\infty} \left[\epsilon \sigma_\infty + e q_D \right]^2. \quad (171)$$

Let $q_D = q_\infty$, we recover the local energy release rate result obtained by Gao et al. [15],

$$J_\ell = \frac{\pi a}{2M} \left(1 + \frac{e^2}{M\epsilon} \right) \left(\sigma_\infty + e E_\infty \right)^2. \quad (172)$$

5.1 Global energy release rate

When a crack grows in a permeable environment, energy release is not only consumed by supplying the surface energy for newly formed crack surfaces, but also consumed by supplying electrostatic energy to the dielectric medium inside the crack. In fact, if surface charge is absent on the crack surfaces, the normal component of electric displacement in piezoelectric medium may equal to the normal component of electric displacement in the dielectric medium inside the crack. This suggests that the crack surface contribution to the J -integral is the part of energy release rate that may go directly into supplying the electrostatic energy increase in the dielectric medium inside the crack. In general, this part of the J -integral contribution relates to the interaction between the dielectric medium inside crack and the fractured piezoelectric material.

By taking into account the contribution of J -integral on crack surface, the so-called global energy release rate can be calculated,

$$J_g = J_\ell + J_{cs}, \quad (173)$$

where J_{cs} denote the energy release contribution from crack surfaces, which can be calculated by

$$J_{cs} = - \int_{cs} n_i D_i \phi_{,X} dS. \quad (174)$$

The normal component of the electric displacement on the crack surfaces along the crack surface and saturation zone is

$$\begin{aligned}
D_Y(X, h_0) &\approx -\epsilon \frac{\partial \psi}{\partial Y} = \left[q_\infty - \frac{\epsilon}{\Delta_c} \left(\bar{M}q_D + \left(\frac{\epsilon_0 r e}{\epsilon} \right) \sigma_\infty \right) \right] \\
&\quad + \frac{\epsilon}{\theta} \frac{1}{\Delta_c} \left[\bar{M}q_D + \left(\frac{\epsilon_0 r e}{\epsilon} \right) \sigma_\infty \right] H(X - a) \\
&= D_{Y1} + D_{Y2} H(X - a),
\end{aligned} \tag{175}$$

where

$$\begin{aligned}
D_{Y1} &:= \left[q_\infty - \frac{\epsilon}{\Delta_c} \left(\bar{M}q_D + \left(\frac{\epsilon_0 r e}{\epsilon} \right) \sigma_\infty \right) \right], \\
D_{Y2} &:= \frac{\epsilon}{\theta} \frac{1}{\Delta_c} \left[\bar{M}q_D + \left(\frac{\epsilon_0 r e}{\epsilon} \right) \sigma_\infty \right].
\end{aligned} \tag{176}$$

The electric potential on crack surfaces may be found as

$$\begin{aligned}
\phi(X, h_0) &\approx \frac{e}{\epsilon \Delta} \left[(\epsilon + \epsilon_0 r) \sigma_\infty + e q_D \right] \sqrt{a^2 - X^2} \left(H(X) - H(X - a) \right) \\
&\quad - \frac{1}{\pi \theta \Delta_c} \left[\bar{M}q_D + \left(\frac{\epsilon_0 r e}{\epsilon} \right) \sigma_\infty \right] \left\{ X \ln \left| \frac{a \sqrt{b^2 - X^2} - X \sqrt{b^2 - a^2}}{a \sqrt{b^2 - X^2} + X \sqrt{b^2 - a^2}} \right| \right. \\
&\quad \left. - a \ln \left| \frac{a \sqrt{b^2 - a^2} - X \sqrt{b^2 - X^2}}{a \sqrt{b^2 - a^2} + X \sqrt{b^2 - X^2}} \right| \right\}.
\end{aligned} \tag{177}$$

Substituting Eq. (175) and Eq. (177) into Eq. (174) yield

$$\begin{aligned}
J_{cs} &= D_{Y1} (\phi(0, 0^+) - \phi(0, 0^-)) + D_{Y2} (\phi(a, 0^+) - \phi(a, 0^-)) \\
&= \frac{2ea}{\Delta_c} \left[(\epsilon + \epsilon_0 r) \sigma_\infty + e q_D \right] \left\{ \frac{q_\infty}{\epsilon} - \frac{1}{\Delta_c} \left(\bar{M}q_D + \left(\frac{\epsilon_0 r e}{\epsilon} \right) \sigma_\infty \right) \right\} \\
&\quad + \frac{4}{\pi \theta} \frac{a}{\Delta_c} \left[\bar{M}q_D + \left(\frac{\epsilon_0 r e}{\epsilon} \right) \sigma_\infty \right] \ln \left| \frac{1 + \sin \theta}{\cos \theta} \right| \\
&\quad \cdot \left\{ \frac{\epsilon}{\Delta_c} \left[\bar{M}q_D + \left(\frac{\epsilon_0 r e}{\epsilon} \right) \right] - q_\infty \right\} \\
&\quad - \frac{4\epsilon a}{\pi \Delta_c^2 \theta^2} \left[\bar{M}q_D + \left(\frac{\epsilon_0 r e}{\epsilon} \right) \sigma_\infty \right]^2 \ln |\sec \theta|,
\end{aligned} \tag{178}$$

where

$$\theta := \cos^{-1} \left(\frac{a}{b} \right).$$

The global energy release rate is then obtained

$$\begin{aligned}
J_g = J_l + J_{cs} &= \frac{\pi a}{2\Delta_c^2} \bar{M} \left[(\epsilon + \epsilon_0 r) \sigma_\infty + eq_D \right]^2 \\
&+ \frac{2ae}{\Delta_c} \left[(\epsilon + \epsilon_0 r) \sigma_\infty + eq_D \right] \left\{ \frac{q_\infty}{\epsilon} - \frac{1}{\Delta_c} \left(\bar{M} q_D + \left(\frac{\epsilon_0 r e}{\epsilon} \right) \sigma_\infty \right) \right\} \\
&+ \frac{4a}{\pi \theta} \frac{1}{\Delta_c} \left[\bar{M} q_D + \left(\frac{\epsilon_0 r e}{\epsilon} \right) \sigma_\infty \right] \ln \left| \frac{1 + \sin \theta}{\cos \theta} \right| \\
&\cdot \left\{ \frac{\epsilon}{\Delta_c} \left[\bar{M} q_D + \left(\frac{\epsilon_0 r e}{\epsilon} \right) \sigma_\infty \right] - q_\infty \right\} - \frac{4a\epsilon}{\pi \Delta_c^2 \theta^2} \left[\bar{M} q_D + \left(\frac{\epsilon_0 r e}{\epsilon} \right) \sigma_\infty \right]^2 \ln |\sec \theta|. \tag{179}
\end{aligned}$$

Consider impermeable limit $\epsilon_0 r = 0$. The global energy release rate becomes

$$\begin{aligned}
J_g &= \frac{\pi a}{2\epsilon \Delta_c} \left[\epsilon \sigma_\infty + eq_D \right]^2 + \frac{2a}{\Delta_c} \left(\frac{e}{\epsilon} \right) \left[\epsilon \sigma_\infty + eq_D \right] (q_\infty - q_D) \\
&- \frac{4a}{\pi \theta \epsilon} q_D (q_\infty - q_D) \ln \left| \frac{1 + \sin \theta}{\cos \theta} \right| - q_D^2 \frac{4a}{\pi \theta^2 \epsilon} \ln |\sec \theta|. \tag{181}
\end{aligned}$$

In the case that there is no charge distribution along the crack surface $q_D = 0$, one may find that

$$J_g = \frac{\pi a}{2\bar{M}} \left(\sigma_\infty^2 + \frac{4e}{\pi} \sigma_\infty q_\infty \right) \tag{182}$$

which may be written in terms of remote stress and electric field,

$$J_g = \frac{\pi a}{2\bar{M}} \left(\frac{M\epsilon + 4e^2/\pi}{M\epsilon + e^2} \sigma_\infty^2 + \frac{4e}{\pi} \sigma_\infty E_\infty \right). \tag{183}$$

This result is similar to the result obtained by the author in a linear analysis of Mode III permeable crack ([40]).

Let $q_D = q_\infty$ in Eq. (181). One may find that

$$J_g = \frac{\pi a}{2\bar{M}} \left(1 + \frac{e^2}{M\epsilon} \right) \left(\sigma_\infty + eE_\infty \right)^2 - \frac{4q_S^2}{\pi \epsilon} a \ln |\sec \theta| \tag{184}$$

which again recovers the result obtained by Gao et al. [15].

6 Crack growth under applied electric load

Extra care should be taken under purely applied electric loading. Assume that there is no remote mechanical load, i.e. $\sigma_\infty = 0$. Let $\epsilon_0 = 0$. The asymptotic fields in front a crack tip, which contains a saturation zone and a layer of positive charge distribution on the crack surfaces, are

$$\epsilon_{YY} = \frac{eq_D}{\Delta_\infty} \frac{X}{\sqrt{X^2 - a^2}} + \frac{e}{\Delta_\infty} (q_\infty - q_D), \tag{185}$$

$$E_Y = -\frac{e^2 q_D}{\epsilon \Delta_\infty} \frac{X}{\sqrt{X^2 - a^2}} + \frac{q_S}{\epsilon} + \frac{e^2}{\epsilon \Delta_\infty} (q_D - q_\infty), \tag{186}$$

$$\sigma_{YY} = \frac{eq_D}{\epsilon} \frac{X}{\sqrt{X^2 - b^2}} + \frac{e}{\epsilon} (q_\infty - q_D - q_S), \tag{187}$$

$$D_Y = q_S, \tag{188}$$

where

$$q_D = \frac{\bar{\theta}}{1 - \bar{\theta}}(q_S - q_\infty). \quad (189)$$

Note that when $q_S > q_\infty \rightarrow q_D > 0$. This excludes any possibility of re-charge. The corresponding energy release rate then becomes

$$J_\ell = \frac{e^2}{\epsilon \Delta_\infty} \left(\frac{\pi a}{2} \right) \left(\frac{\bar{\theta}}{1 - \bar{\theta}} \right) (q_S - q_\infty)^2 > 0. \quad (190)$$

This suggests that under purely applied electric load crack growth is possible. However, the global energy release rate paints a slightly different picture,

$$J_g = \frac{2a}{\Delta_c} \left(\frac{e^2}{\epsilon} \right) q_D q_\infty - \frac{4a}{\pi \theta \epsilon} q_D q_\infty \ln \left| \frac{1 + \sin \theta}{\cos \theta} \right| \\ - \left(2 - \frac{\pi}{2} \right) \frac{ae^2}{\epsilon \Delta_c} q_D^2 + \frac{4a}{\pi \theta \epsilon} q_D^2 \ln \left| \frac{1 + \sin \theta}{\cos \theta} \right| - q_D^2 \frac{4a}{\pi \theta^2 \epsilon} \ln |\sec \theta|.$$

Note that when $\theta \ll 1$,

$$\ln \left| \frac{1 + \sin \theta}{\cos \theta} \right| = \theta + \frac{1}{6} \theta^3 + \frac{5}{12} \theta^4 + \dots \quad (191)$$

The global energy release rate may then be negative, if $q_D < 1$. This result suggests that under purely electric load, the global energy release rate criterion is sensitive to charge distribution on the crack surfaces, even though the local energy release rate indicates the propensity to fracture.

This may help to explain the scattered nature of experimental data on fracture under electric load (see discussions in [27]).

7 Conclusions

In this paper, the combined effects of domain switching, permeability, and surface charge distribution are taken into account to study crack growth in a piezoelectric ceramic.

The analyses presented in this paper clearly show that the surface charge on a permeable crack surfaces due to any possible charge-discharge mechanisms is a crucial element to link applied electric field to crack driven force. Based on the analyses presented in this paper, it is clear that the surface charge on a permeable crack surfaces due to any possible charge-discharge mechanisms may either shield or assist energy-moment flux flow into or flow out the dielectric medium inside a crack, which manifests the important role of the applied electric field in crack growth.

It has been an outstanding problem regarding the energy release rate of a piezoelectric crack. The impermeable crack solution always leads to negative energy release rate, giving a false impression that applied electric field will prohibit crack growth. The fallacy of impermeable approximation is that it artificially impose a re-charge process, which shields and may even reverse the direction of energy-momentum flux at crack surfaces. In reality, the permeable crack provides a leaky mode allowing applied electric field pass through. Therefore, by accounting the interaction between dielectric medium inside a crack and the piezoelectric solids, the global energy release rate provide a unique criterion to measure the fracture toughness of a piezoelectric material.

It is shown that fracture toughness measurement based on the saturation strip model is a complex subject depending on several different parameters, namely, saturation, charge distribution, and permeability. The global energy release rate also depends on several different parameters as well.

It has found that at impermeable limit without surface charge distribution ($q_D = 0$) the global energy release rate derived for a permeable crack is in a broad agreement with the known experimental observations (e.g. [12], [13]), which is in contrast with the local energy release rate criterion proposed by Gao et al. [14], [15] according to the strip-saturation model.

In general, it has been shown that fracture toughness measurement based on the permeable saturation strip model is a complex subject depending on several different parameters, namely, saturation, charge distribution, and permeability. The global energy release rate also depends on several different parameters as well. Especially, under purely electric load, the global energy release rate changes its sign depending on the surface charge distribution. An in-depth study is needed to investigate the roles of electric load, surface charge distribution, saturation, and their interactions.

Acknowledgements

The author would like to acknowledge the support from the Academic Senate Committee on Research at University of California (Berkeley) through the fund of BURNL-07427-11503-EGSLI.

References

- [1] Pak, Y. E.: Crack extension force in a piezoelectric material. *J. Appl. Mech.* **57**, 647–653 (1990).
- [2] Pak, Y. E.: Linear electro-elastic fracture mechanics of piezoelectric materials. *Int. J. Fract.* **54**, 79–100 (1992).
- [3] Li, S., Cao, W., Cross, L. E.: Stress and electric displacement distribution near Griffith's type III crack tips in piezoceramics. *Mater. Lett.* **10**, 219–222 (1990).
- [4] Sosa, H. A.: Three-dimensional eigenfunction analysis of a crack in a piezoelectric material. *Int. J. Solids Struct.* **26**, 1–15 (1990).
- [5] Sosa, H. A.: Plane problems in piezoelectric media with defects. *Int. J. Solids Struct.* **28**, 491–505 (1991).
- [6] Suo, Z., Kuo, C.-M., Barnett, D. M., Willis, J. R.: Fracture mechanics for piezoelectric ceramics. *J. Mech. Phys. Solids* **40**, 739–765 (1992).
- [7] Suo, Z.: Models for breakdown-resistant dielectric and ferroelectric ceramics. *J. Mech. Phys. Solids* **41**, 1155–1176 (1993).
- [8] Dunn, M. L.: The effects of crack face boundary conditions on the fracture mechanics of piezoelectric solids. *Engng. Fract. Mech.* **48**, 25–39 (1994).
- [9] Dascalu, C., Maugin, G. A.: Energy-release rates and path-independent integrals in electroelastic crack propagation. *Int. J. Engng. Sci.* **32**, 755–765 (1994).
- [10] Dascalu, C., Maugin, G. A.: On the dynamic fracture of piezoelectric materials. *Q. J. Mech. Appl. Math.* **48**, 237–255 (1995).
- [11] Dascalu, C., Maugin, G. A.: On the electroelastic fracture. *ZAMP* **46**, 355–365 (1995).
- [12] Park, S., Sun, C. T.: Fracture criteria for piezoelectric ceramics. *J. Am. Ceram. Soc.* **78**, 1475–1480 (1995).
- [13] Park, S., Sun, C. T.: Effect of electric field on fracture of piezoelectric ceramics. *Int. J. Fract.* **70**, 203–216 (1995).
- [14] Gao, H., Barnett, D. M.: An invariance property of local energy release rates in a strip saturation model of piezoelectric fracture. *Int. J. Fract.* **44**, R25–R29 (1996).

- [15] Gao, H., Zhang, T.-Y., Tong, P.: Local and global energy release rates for an electrically yielded crack in a piezoelectric ceramic. *J. Mech. Phys. Solids* **45**, 491–510 (1997).
- [16] Lynch, C. S., Yang, W., Suo, Z., McMeeking, R. M.: Electric field induced cracking in ferroelectric ceramics. *Ferroelectrics* **166**, 11–30 (1995).
- [17] Lynch, C. S., Chen, L., Suo, Z., McMeeking, R. M., Yang, W.: Crack growth in ferroelectric ceramics driven by cyclic polarization switching. *J. Intell. Mater. Sys. Struct.* **6**, 191–198 (1995).
- [18] Zhang, T.-Y., Hack, J. E.: Mode-III crack in piezoelectric materials. *J. Appl. Phys.* **71**, 5865–5870 (1992).
- [19] Fulton, C. C., Gao, H.: Effect of local polarization switching on piezoelectric fracture. *J. Mech. Phys. Solids* **49**, 927–952 (2001).
- [20] Ru, C. Q., Mao, X., Epstein, M.: Electric-field induced interfacial cracking in multilayer electric actuators. *J. Mech. Phys. Solids* **46**, 1301–1318 (1998).
- [21] Ru, C. Q.: Effect of electrical polarization saturation on stress intensity factors in a piezoelectric ceramic. *Int. J. Solids Struct.* **36**, 869–883 (1999).
- [22] Yang, W., Zhu, T.: Fracture and fatigue of ferroelectric under electric and mechanical loading. *Fatigue Fract. Engng. Mater. Struct.* **21**, 1361–1369 (1998).
- [23] Yang, W., Zhu, T.: Switch-toughening of ferroelectric subjected to electric field. *J. Mech. Phys. Solids* **46**, 291–311 (1998).
- [24] Zhu, T., Yang, W.: Toughness variation of ferroelectrics by polarization switch under nonuniform electric field. *Acta Mater.* **45**, 4695–4702 (1997).
- [25] Zhang, T.-Y., Tong, P.: Fracture mechanics for a mode III-crack in a piezoelectric material. *Int. J. Solids Struct.* **33**, 343–359 (1996).
- [26] Zhang, T.-Y., Qian, C.-F., Tong, P.: Linear electro-elastic analysis of a cavity or a crack in a piezoelectric material. *Int. J. Solids Struct.* **35**, 2121–2149 (1998).
- [27] Zhang, T.-Y., Zhao, M., Tong, P.: Fracture of piezoelectric ceramics. In: *Adv. Appl. Mech.* **38** (von der Giessen, E., Wu, T. Y., eds.), pp. 147–289. Academic Press 2001.
- [28] Zhu, T., Fang, F., Yang, W.: Fatigue crack growth in ferroelectric ceramic below the coercive field. *J. Mater. Sci. Letters* **18**, 1025–1027 (1999).
- [29] Zhu, T., Yang, W.: Fatigue crack growth in ferroelectric driven by cyclic electric loading. *J. Mech. Phys. Solids* **47**, 81–97 (1999).
- [30] Sun, C. T., Jiang, L. Z.: Domain switching induced stress at the tip of a crack in piezoceramics. In: *Smart materials and structures* (Tomlinson, G. R., Bullough, W. A., eds.), pp. 715–722. Proc. 4th European and 2nd MIMR Conference, Harrogate, UK. Bristol and Philadelphia: Institute of Physics Publishing 1998.
- [31] Mehta, K., Virkar, A. V.: Fracture mechanisms in ferroelectric-ferroelastic lead zirconate titanate (Zr:ti = 0.54:0.46) ceramics. *J. Amer. Ceram. Soc.* **73**, 567–574 (1990).
- [32] Tobin, A., Pak, Y. E.: Effects of electric fields on fracture behavior of PZT ceramics. *Smart structures and materials 1916*, pp. 78–86. Proc. SPIE, 1993.
- [33] Cao, H. C., Evans, A. G.: Electric-field-induced fatigue crack growth in piezoelectric ceramics. *J. Am. Ceram. Soc.* **77**, 1783–1786 (1994).
- [34] Tiersten, H. F.: *Linear piezoelectric plate vibrations*. New York: Plenum Press 1969.
- [35] Rice, J. R., Ben-Zion, Y., Kim, K. S.: Three-dimensional perturbative solution for a dynamic planar crack moving unsteadily in a model elastic solid. *J. Mech. Phys. Solids* **43**, 813–843 (1994).
- [36] Erdélyi, A., Magnus, W., Oberhettinger, F., Tricomi, F. G.: *Tables of integral transforms*. Based in part on notes left by Harry Bateman, vol. 1–2. New York: McGraw-Hill 1954.
- [37] Lighthill, M. J.: *Introduction to fourier analysis and generalized functions*. Cambridge: Cambridge University Press 1958.
- [38] Sneddon, I. N., Lowengrub, M.: *Crack problems in the classical theory of elasticity*. New York: Wiley 1969.
- [39] Cherepanov, G. P.: *Mechanics of brittle fracture*. New York: McGraw-Hill 1979.
- [40] Li, S.: On global energy release rate of a permeable crack in a piezoelectric ceramic. *J. Appl. Mech.* **70**, 246–252 (2003).

Author's address: S. Li, Department of Civil and Environmental Engineering, University of California, Berkeley, California, U.S.A. (E-mail: li@ce.berkeley.edu)